

# Comparison of spin-echo echoplanar imaging and gradient recalled echo-based MR elastography at 3 Tesla with and without gadoxetic acid administration

Yong Seek Kim<sup>1</sup> · Ji Soo Song<sup>1,2,3</sup>  · Stephan Kannengiesser<sup>4</sup> · Seung Young Seo<sup>2,3,5</sup>

Received: 31 August 2016 / Revised: 11 December 2016 / Accepted: 16 February 2017 / Published online: 13 March 2017  
© European Society of Radiology 2017

## Abstract

**Objective** To compare spin-echo echoplanar imaging (SE-EPI) and gradient recalled echo (GRE) MR elastography (MRE) at 3 T with and without gadoxetic acid administration. **Methods** We included 84 patients who underwent MRE before and after gadoxetic acid administration, each time using SE-EPI and GRE sequences. Diagnostic performance for predicting clinical liver cirrhosis and high-risk oesophageal varices was assessed using the area under the receiver-operating characteristic curve (AUC). The relationships between T2\* and success of MRE, and correlations of liver stiffness (LS) values between the two sequences or before and after gadoxetic acid administration, were investigated. **Results** SE-EPI-MRE resulted in a significantly lower failure rate than GRE-MRE (1.19% vs. 10.71%,  $P = 0.018$ ). Increased T2\* was related to higher probability of successful LS measurement (odds ratio, 1.426;  $P = 0.004$ ). The AUC of SE-EPI-MRE was comparable to that of GRE-MRE for the

detection of clinical liver cirrhosis (0.938 vs. 0.948,  $P = 0.235$ ) and high-risk oesophageal varices (0.839 vs. 0.752,  $P = 0.354$ ). LS values were not significantly different before and after gadoxetic acid administration.

**Conclusion** SE-EPI-MRE can substitute for GRE-MRE for the detection of clinical liver cirrhosis and high-risk oesophageal varices. SE-EPI-MRE is particularly useful in patients with iron deposition, with lower failure rates than GRE-MRE.

## Key Points

- LS values are comparable between SE-EPI-MRE and GRE-MRE.
- Administration of gadoxetic acid does not influence LS measurement.
- The failure rate of SE-EPI-MRE is significantly lower than that of GRE-MRE.

**Keywords** Magnetic resonance elastography · Liver fibrosis · Spin echo · Gradient recalled echo · Gadaxetic acid

✉ Ji Soo Song  
pichgo@gmail.com

- <sup>1</sup> Department of Radiology, Chonbuk National University Medical School and Hospital, 20 Geonji-ro, Deokjin-gu, Jeonju, Chonbuk 54907, Korea
- <sup>2</sup> Research Institute of Clinical Medicine of Chonbuk National University, 20 Geonji-ro, Deokjin-gu, Jeonju, Chonbuk 54907, Korea
- <sup>3</sup> Biomedical Research Institute of Chonbuk National University Hospital, 20 Geonji-ro, Deokjin-gu, Jeonju, Chonbuk 54907, Korea
- <sup>4</sup> MR Applications Development, Siemens Healthcare, Erlangen, Germany
- <sup>5</sup> Department of Internal Medicine, Chonbuk National University Medical School and Hospital, Jeonju, Korea

## Abbreviations

LS Liver stiffness  
MRE Magnetic resonance elastography  
SE-EPI Spin-echo echoplanar imaging

## Introduction

The detection, staging and monitoring of liver fibrosis is of great clinical importance for the management of patients with chronic liver disease, because liver fibrosis is used to evaluate the severity of the underlying chronic liver disease, guide treatment decisions, assess disease outcomes and evaluate response to therapy [1]. Although percutaneous liver biopsy is still considered the reference standard for liver fibrosis

measurements, it has several limitations such as invasiveness, risks of complications such as haemorrhage and infection, sampling error and intra- and interobserver variations of interpretation [2]. As a result, MR elastography (MRE) is gaining acceptance as a non-invasive tool for the assessment of liver fibrosis through head-to-head comparisons with histopathologic data [3–7]. MRE also demonstrates superior diagnostic performance and reliability compared to other non-invasive tools such as MR imaging features, ultrasound elastography or biochemical testing [4, 8–11]. As a result, the clinical use of MRE in patients with chronic liver disease is increasing [12–15].

Most published clinical liver MRE studies used gradient recalled echo (GRE) sequences on 1.5-T or 3-T MR systems to encode shear wave propagation through motion-sensitizing gradients and phase-sensitive acquisition [2]. In GRE-based MRE (GRE-MRE), both repetition time (TR) and echo time (TE) are greater than the vibration period of the active driver (typically  $1/60$  Hz = 16.7 ms). This results in considerable signal dephasing in tissues with short transverse relaxation times [16]. Therefore, most failures of GRE-MRE are caused by the short  $T2^*$  transverse relaxation time of iron-overloaded liver [2, 6, 17]. Considering that the liver exhibits faster  $T2^*$  relaxation at 3 T than at 1.5 T, the failure risk of GRE-MRE is increased for iron-overloaded patients at 3 T. An alternative approach to overcome this limitation is to use spin-echo-based echoplanar imaging (SE-EPI-MRE), which is less sensitive to transverse relaxation signal decay than GRE-MRE is. A high degree of accuracy, reproducibility and measurement repeatability are needed to foster the widespread application of MRE in clinical use. Multiple published studies demonstrated that liver stiffness (LS) measured using MRE is not significantly influenced by technical factors such as MR platform, observer or gadolinium administration [18–22]. However, the effect of the MR sequence on LS measurements has rarely been examined [17, 23, 24]. In addition, the effects of gadoxetic acid administration on LS measured at 3 T SE-EPI-MRE or GRE-MRE have not been reported. In this context, the purpose of this study was to compare the diagnostic performances of 3-T SE-EPI-MRE, 3-T GRE-MRE and serum fibrosis markers for predicting clinical liver cirrhosis and high-risk oesophageal varices, and to evaluate the effects of gadoxetic acid administration at 3 T on SE-EPI-MRE and GRE-MRE.

## Materials and methods

### Patients

The institutional review board of our institution approved this retrospective study, and the requirement for patient informed consent was waived. Between April 2015 and September 2015, 90 patients underwent gadoxetic acid-enhanced liver

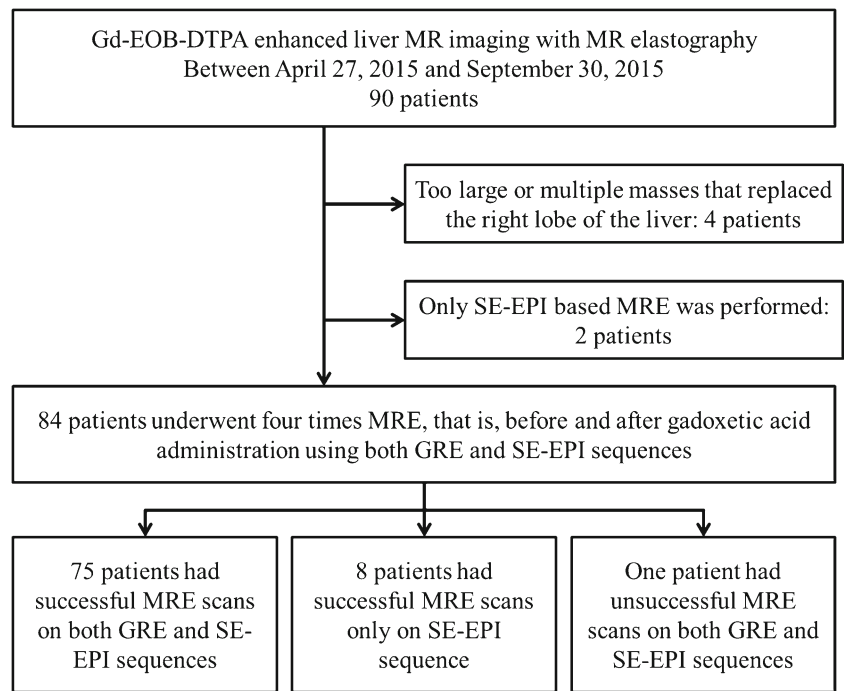
MRI with MRE at our institution. Among the 90 patients, we excluded four patients with too large or too many hepatic masses to allow the placement of a region of interest (ROI) in the liver parenchyma, and two patients who had undergone only SE-EPI-MRE. Therefore, the study sample included 84 patients (56 men, 28 women; mean age, 58.7 years; range, 33–81 years). MRE was performed four times per patient using the two sequences, i.e. before (precontrast) and after (postcontrast) gadoxetic acid administration with GRE and SE-EPI (Fig. 1).

Patients who had undergone successful MRE scans in at least one sequence were categorized into two groups according to the presence (liver cirrhosis group,  $n = 46$ ) or absence (non-liver cirrhosis group,  $n = 37$ ) of liver cirrhosis. Since the main purpose of this study was to evaluate the effects of MR sequence and gadoxetic acid on LS measurements, the diagnoses of liver cirrhosis were established clinically by complete medical history, physical examination, biochemical tests and morphologic imaging findings. The aetiologies of liver cirrhosis in our sample were viral hepatitis B ( $n = 32$ ) and C ( $n = 2$ ), alcohol-induced hepatitis ( $n = 11$ ) or an unknown cause ( $n = 1$ ).

We obtained information regarding results of biochemical tests and oesophagogastroduodenoscopy (EGD) by reviewing medical records to compare their diagnostic performance for predicting liver cirrhosis or oesophageal varices between MRE and serum fibrosis markers such as aspartate aminotransferase to platelet ratio index (APRI) and fibrosis index based on the four factors (FIB-4). All biochemical test results were obtained within 1 month of the MR examination. Of the 46 liver cirrhosis patients, 31 underwent EGD for variceal screening within 3 months before or after MR examination. Oesophageal varices were graded as follows: grade 0 = no varices; grade 1 = small straight varices; grade 2 = enlarged tortuous varices occupying less than one third of the lumen; grade 3 = large coil-shaped varices occupying more than one third of the lumen [13].

### MRI examination

All MR examinations were performed on a 3-T MR scanner (Magnetom Skyra, Siemens Healthcare GmbH, Erlangen, Germany) using the 18-element body matrix and 4–12 elements of the integrated spine matrix coils. The routine liver MR protocol consisted of the following sequences: breath-hold axial and coronal T2-weighted half-Fourier acquisition single-shot turbo-spin-echo, axial T1-weighted dual-echo (in-phase and opposed-phase), respiratory triggered T2-weighted fast-spin-echo with fat suppression, T1-weighted GRE with fat-suppression before and after the injection of contrast agent, and free-breathing diffusion-weighted imaging using single-shot EPI. Dynamic imaging and hepatobiliary phase imaging were performed with injections of gadoxetic acid (Primovist;

**Fig. 1** Flow chart of the study sample

Bayer Healthcare, Berlin, Germany). Of the 84 patients in the sample, 52 patients suspected of having diffuse liver disease on the basis of dual-ratio Dixon discrimination [25] underwent multistep adaptive fitting with multi-echo MRI [26, 27].

## MRE examination

### GRE based MRE

The 60-Hz acoustic wave was delivered by an active driver (Resoundant Inc., Rochester, MN, USA). A passive cylindrical driver of 19 cm diameter and 1.5 cm thickness was placed against the right chest wall over the liver at the level of the xiphoid process. Then, propagation of shear waves in the liver was produced by transmitting continuous acoustic vibrations from the active driver to the passive driver through a flexible vinyl tube. Three slices of MRE were obtained for each patient, and each slice required 18-s breath-holds at the end-expiratory period. When acquisition was completed, the wave images were automatically processed by the MR scanner and images depicting tissue stiffness (elastograms) quantitatively in units of kilopascals (kPa) were generated. In addition, the scanner software produces confidence maps to exclude areas of unreliable results, which may be caused by artefacts such as significant wave interference or oblique wave propagation, and elastograms with 95% confidence threshold were produced.

### SE-EPI based MRE

The same wave generation setup was used as in GRE-based MRE. A prototype 2-dimensional SE-EPI sequence was used. Three slices with the same positions as in the GRE acquisition were obtained in a single 7-s breath-hold at the end-expiratory period. Elastograms and confidence maps were generated using the same scanner software as for GRE-MRE.

Post-contrast MRE using both GRE and SE-EPI was conducted in the same manner during the time period between the 10 min and 20 min hepatobiliary phase imaging. The details of MRE scan parameters are summarized in Table 1.

**Table 1** MR parameters used for MRE acquisition

	SE-EPI	GRE
TR/TE (ms)	600/48	50/22
FOV (cm)	38	38
Matrix	128 × 104	128 × 96
Number of slices	3	3
Slice thickness (mm)	5	5
Flip angle (degree)	90	25
Motion encoding direction	z	z
Parallel imaging acceleration factor (GRAPPA)	2	3
Acquisition time	7 s	54 s (18 s × 3 slices)

TR repetition time, TE echo time, MEG motion encoding gradient, GRAPPA generalized autocalibrating partially parallel acquisitions

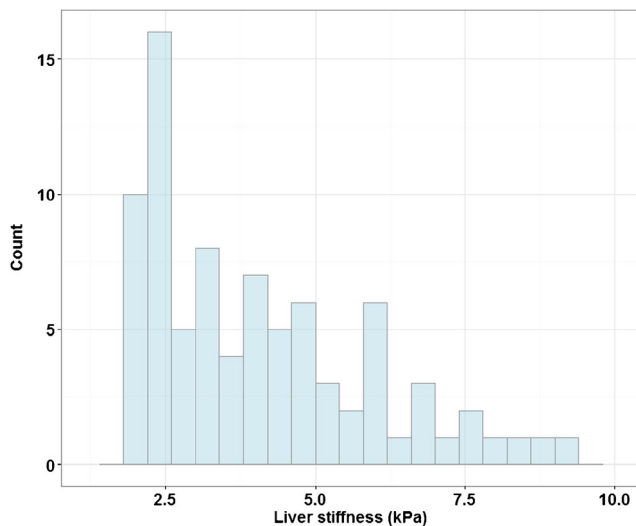


**Fig. 2** Histogram shows a positively skewed distribution of liver stiffness in the 83 successful precontrast SE-EPI-MREs

### Imaging analysis

All MRE examinations were interpreted by one radiologist with 9 years of experience in liver MR imaging. The mean shear stiffness of the liver was calculated by placing manually specified ROIs into the stiffness maps of MRE images. Three circular ROIs of 1–2 cm diameter were drawn in three contiguous slices of confidence maps (total of nine ROIs) in the hepatic parenchyma excluding major blood vessels, liver edges and motion artefacts. To evaluate the interobserver agreement of LS measurements, another radiologist with 4 years of experience in liver MR imaging measured the values in the same manner for the 83 successful precontrast SE-EPI-MREs. To estimate hepatic iron content, three ROIs were placed on a corresponding  $R2^*$  map of the multistep adaptive fitting approach with multi-echo MRI at main portal vein level.  $T2^*$  was calculated as the reciprocal of  $R2^*$  ( $T2^* = 1/R2^*$ ) [25].

### Review of failures

All cases rated as failed by the radiologists were reviewed for potential causes in consensus by one radiologist with 9 years of experience in liver MR imaging and a technical expert with 4 years of experience with MRE.

### Statistical analyses

All statistical analyses were performed using R software (version 3.2.4; <http://www.R-project.org>). Continuous variables were described as medians with interquartile ranges (IQRs); possible differences between groups were tested by Mann–Whitney  $U$  tests. Interobserver agreement was measured using the intraclass correlation coefficient (ICC). A receiver

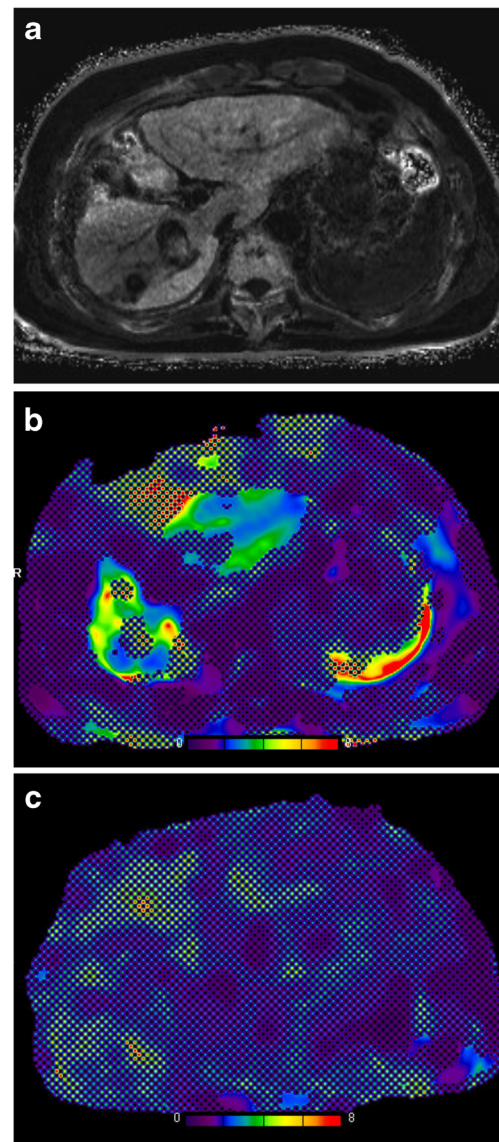


**Fig. 3** An example of GRE-MRE failure due to iron overload in a 71-year-old man with alcoholic liver cirrhosis and hepatocellular carcinoma. **a** On the  $R2^*$  map,  $T2^*$  value was calculated to be 5 ms, which indicates mild to moderate iron overload. **b** The precontrast SE-EPI-MRE (95% confidence map) shows increased LS value of 3.13 kPa in the right lobe of the liver. **c** The precontrast GRE-MRE (95% confidence map) shows no measurable area

operating characteristic (ROC) curve was generated for the LS value measured via the two MRE sequences, APRI and FIB-4, and to determine the optimal cut-off for the detection of clinical liver cirrhosis and identification of high-risk oesophageal varices. The area under the ROC curve (AUC) was calculated as a measure of diagnostic performance. The sensitivity and specificity were also calculated. Fisher's exact test was used to determine whether the failure rates were different between the two MRE sequences. The relationship between  $T2^*$  and successful LS measurement was tested using logistic regression analysis with the calculation of odds ratios with 95% confidence intervals (CI). The difference between LS

before and after gadoteric acid administration was analysed using paired *t* tests. Correlations of LS between the two sequences or before and after gadoteric acid administration were analysed by Pearson's correlation coefficient analysis and Bland–Altman plots in 75 patients who had successful MRE scans using both SE-EPI and GRE sequences. *P* values less than 0.05 were considered to indicate significant differences.

## Results

### Distribution of liver stiffness measurements and interobserver agreement

The median value of LS in the 83 successful precontrast SE-EPI-MREs was 3.47 kPa (range, 1.90–9.12; IQR, 2.44–5.01) with a broad positively skewed distribution (Fig. 2). The interobserver agreement of the two radiologists was excellent, with ICC of 0.911.

### Diagnostic performances of MRE and serum fibrosis markers in detecting clinical liver cirrhosis

The diagnostic performance of MRE ( $AUC_{GRE} = 0.948$ ;  $AUC_{SE-EPI} = 0.938$ ) was superior to that of serum fibrosis markers ( $AUC_{APRI} = 0.914$ ;  $AUC_{FIB-4} = 0.915$ ) for identifying clinical liver cirrhosis, resulting in higher sensitivity (92.3% and 95.7% for GRE and SE-EPI vs. 84.8% and 94.4% for

APRI and FIB-4) while maintaining specificity (94.3% and 88.9% for GRE and SE-EPI vs. 94.4% and 77.8% for APRI and FIB-4). Although GRE-MRE had slightly higher AUC than SE-EPI-MRE, the values were not significantly different ( $P = 0.235$ ). The optimal cut-off value based on the ROC curve was as follows: GRE, 3.03 kPa; SE-EPI, 3.06 kPa; APRI, 0.603; FIB-4, 1.833.

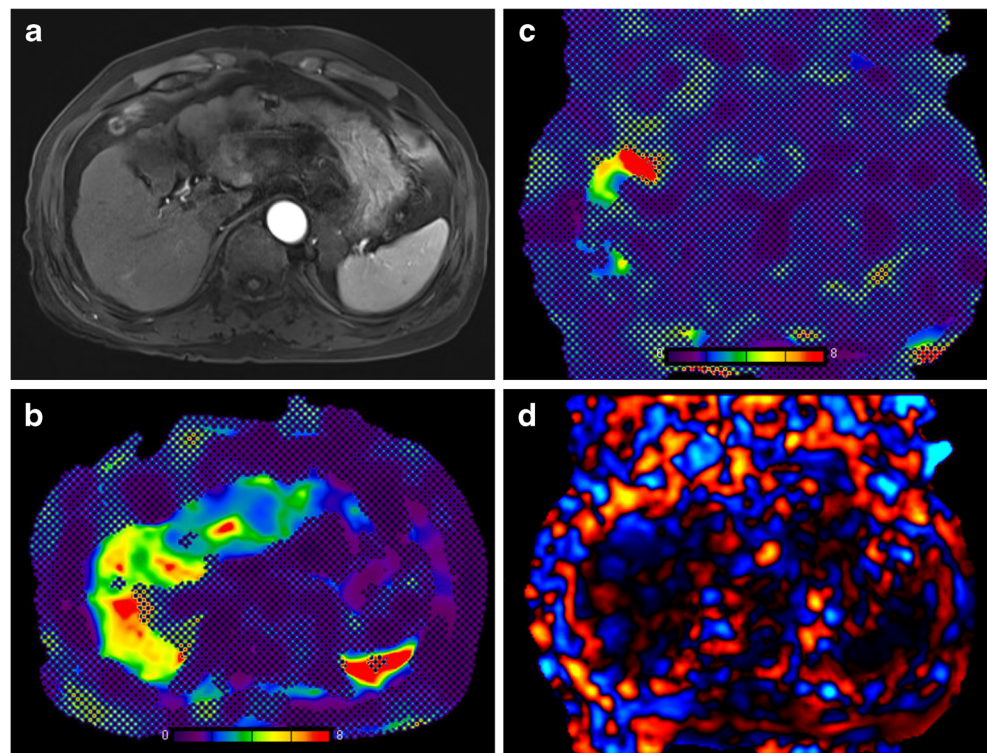
### Diagnostic performances of MRE and serum fibrosis markers in discriminating high-risk varices

Fifteen patients had oesophageal varices (grade 1 = 8 patients; grade 2 = 7 patients). Patients were divided into two groups: a low-risk group (grade 0–1 = 24 patients) and a high-risk group (grade 2–3 = 7 patients). In discriminating high-risk varices ( $\geq$ grade 2), SE-EPI-MRE showed higher diagnostic performance ( $AUC = 0.839$ ) than GRE-MRE, APRI and FIB-4 ( $AUC = 0.752$ , 0.702 and 0.780, respectively), but did not reach significance ( $P > 0.05$ ). The optimal cut-off value based on the ROC curve was as follows: GRE, 4.493 kPa; SE-EPI, 5.880 kPa; APRI, 1.293; FIB-4, 4.815. It should be noted that of the 31 patients who underwent EGD, five patients were excluded when generating the ROC curve of GRE-MRE because of failures in GRE-MRE.

### Failures

SE-EPI-MRE failed in one patient (1.19%) and GRE-MRE failed in nine patients (10.71%,  $P = 0.018$ ). Eight of nine

**Fig. 4** An example of GRE-MRE failure due to poor wave propagation posed by anterior interposition of the colon and visceral fat to the liver in a 52-year-old man with chronic hepatitis B-associated liver cirrhosis and hepatocellular carcinoma. The  $T2^*$  value was calculated to be 20.8 ms, which indicates no iron overload (not shown). **a** Arterial phase of T1 weighted GRE fat-suppressed image shows anterior interposition of the colon and peritoneal fat to the liver. **b** The precontrast SE-EPI-MRE (95% confidence map) shows increased LS value of 3.27 kPa in the right lobe of the liver. **c** The precontrast GRE-MRE (95% confidence map) shows an insufficient measurable area. **d** A GRE-MRE wave image shows poor wave propagation



patients with GRE-MRE failure underwent liver MRI for follow-up of chronic liver disease. Six of nine patients with GRE-MRE failure had a short  $T2^*$ , indicating elevated iron deposition (Fig. 3), while the remaining three failures were mainly due to poor encoding of wave propagation (Fig. 4). The patient-specific causes of poor wave propagation were anterior interposition of visceral fat and colon to the liver ( $n=2$ ) and poor image phase SNR ( $n=1$ ). There were no cases of failure due to respiratory motion artefacts.

### Relationship between successful LS measurement on GRE-MRE and hepatic iron content

Of 52 patients who underwent multistep adaptive fitting approach with multi-echo MRI for hepatic iron quantification, 44 and 8 patients had successful and failed GRE-MRE, respectively. The median  $T2^*$  of the failure group was significantly lower (8.84 ms; IQR, 4.44–20.00) than that of the success group (22.48 ms; IQR, 19.62–25.98;  $P=0.001$ ; Fig. 5a). On the basis of logistic regression analysis, increased  $T2^*$  was related to higher probability of successful LS measurement (odds ratio, 1.426; 95% CI, 1.185–1.974;  $P=0.004$ ; Fig. 5b).

### Correlations between SE-EPI and GRE-MRE

The measured LS values ranged from 1.90 kPa to 9.12 kPa (median, 3.47 kPa; IQR, 2.44–5.01) and 1.78 kPa to 9.92 kPa (median, 3.33 kPa; IQR, 2.36–5.20) for precontrast and postcontrast SE-EPI-MRE. LS values for GRE sequences ranged from 1.62 kPa to 10.06 kPa (median, 3.17 kPa; IQR, 2.17–4.91) and 1.70 kPa to 10.38 kPa (median, 3.25 kPa; IQR, 2.13–4.64) for precontrast and postcontrast GRE-MRE. LS values were not significantly different between precontrast SE-EPI and precontrast GRE-MRE, with a correlation coefficient of 0.951 ( $P<0.0001$ ). Bland–Altman 95% limits of agreement (LOA) between precontrast SE-EPI and precontrast GRE-MRE are depicted in Fig. 6a.

After gadoxetic acid administration, the correlation coefficient between postcontrast SE-EPI and postcontrast GRE-MRE was 0.967 ( $P<0.0001$ ). Bland–Altman 95% LOA between postcontrast SE-EPI and postcontrast GRE-MRE is depicted in Fig. 6a.

### Correlations between pre- and postcontrast MRE

No significant differences were observed between LS values measured before and after gadoxetic acid administration (SE-EPI-MRE,  $P=0.296$ ; GRE-MRE,  $P=0.714$ ). The correlation coefficients were 0.976 ( $P<0.0001$ ) and 0.987 ( $P<0.0001$ ) for SE-EPI-MRE and GRE-MRE, respectively. Bland–Altman 95% LOA between precontrast and postcontrast SE-EPI-MRE and GRE-MRE is depicted in Fig. 6b.

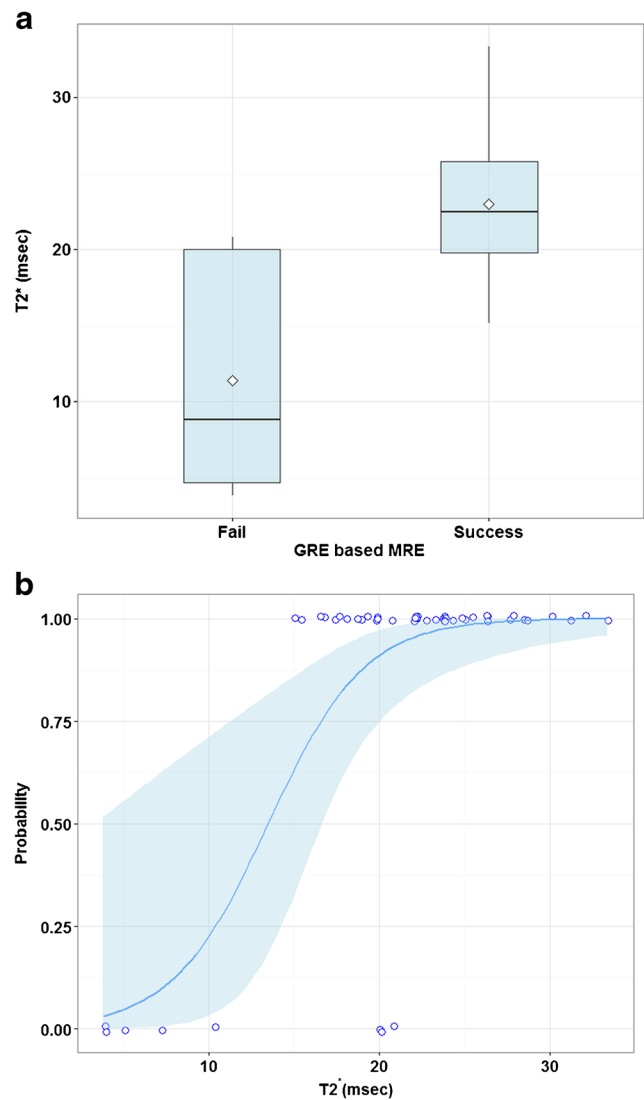


**Fig. 5** **a** Box and whisker plot shows distribution of  $T2^*$  in patients with failure and success of GRE-MRE. Median  $T2^*$  value was significantly lower in patients with failure ( $P=0.001$ ). **b** The graph shows predicted probabilities of successful measurement as a function of  $T2^*$ . Light blue shaded area indicates 95% confidence interval. Increased  $T2^*$  was associated with significantly higher probability of successful measurement ( $P=0.004$ )

## Discussion

In our study, two MRE sequences each were performed for 84 patients at 3 T, showing excellent correlations in LS values between SE-EPI-MRE and GRE-MRE. The diagnostic accuracy of SE-EPI-MRE was not inferior to that of GRE-MRE for the detection of clinical liver cirrhosis and high-risk oesophageal varices. Also of note is that SE-EPI-MRE was successful for most cases in which GRE-MRE failed. The results provide motivation for converting existing 3-T MR systems that currently use GRE-MRE to SE-EPI-MRE because this will provide a considerable improvement in technical success rates.

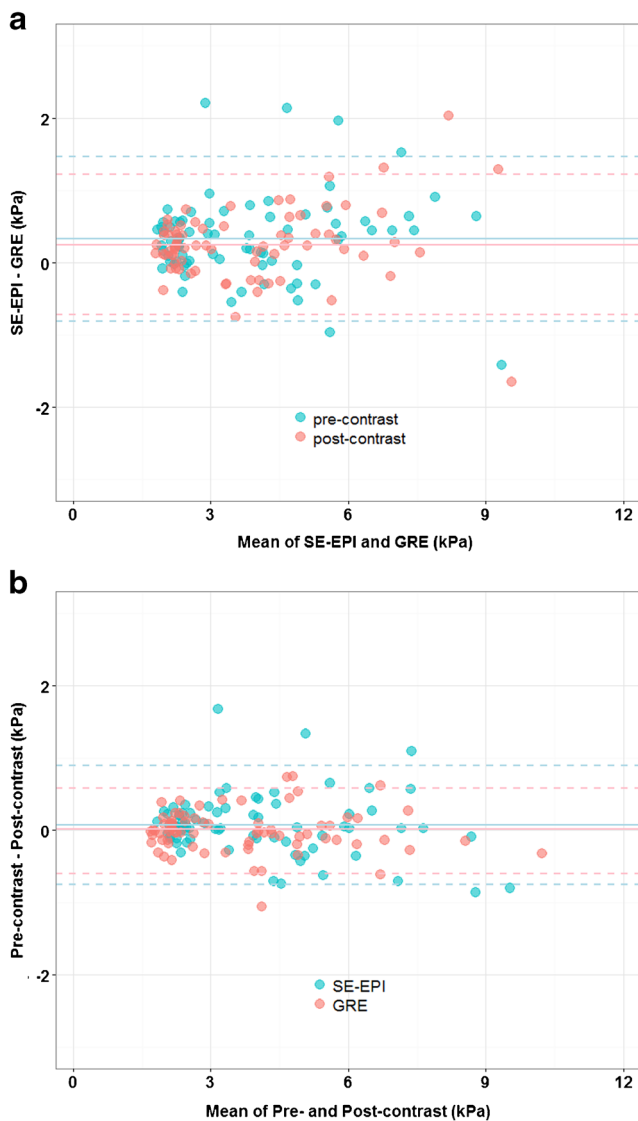


**Fig. 6** **a** Bland–Altman plots showing distributions of differences against the means of SE-EPI and GRE-MRE. Mean difference (*solid line*) was 0.33 and 0.25 for precontrast and postcontrast MRE, respectively. 95% LOA (*dashed line*) was  $-0.81$  kPa to  $1.47$  kPa and  $-0.72$  kPa to  $1.22$  kPa for precontrast and postcontrast MRE, respectively. **b** Bland–Altman plots showing distributions of differences against the means of precontrast and postcontrast MRE. Mean difference (*solid line*) was 0.07 and 0.01 for SE-EPI and GRE sequences, respectively. The 95% LOA (*dashed line*) was  $-0.76$  kPa to  $0.90$  kPa and  $-0.60$  kPa to  $0.58$  kPa for SE-EPI and GRE sequences, respectively

This study is also unique in showing the effects of gadoxetic acid on 3-T MRE. The paramagnetic effects of gadoxetic acid may affect the phase changes of protons in the liver [18]. In previous studies, it had been shown that LS values measured by 1.5-T GRE-MRE did not differ before and after administration of gadoxetic acid or gadopentetic acid [18, 22]. In our study, the lack of influence of gadoxetic acid on the measured LS was confirmed and extended to 3-T SE-EPI-MRE and GRE-MRE, while gadoxetic acid-induced phase changes were not

investigated. On the basis of our results, either SE-EPI-MRE or GRE-MRE could be implemented between the 10 min and 20 min hepatobiliary phase sequences of gadoxetic acid-enhanced MRI. In the context of our daily practice environment, with limited time for each MR examination, MRE can thus be advantageously carried out without requiring additional examination time.

Multiple investigations have shown that MRE has superior diagnostic performance compared to other non-invasive methods [4, 8–11]. Consistent with these previous studies, MRE in our study had similarly high diagnostic accuracy compared to APRI and FIB-4. However, the cut-off values of MRE for detection of liver cirrhosis in our study were lower (GRE, 3.03 kPa; SE-EPI, 3.06 kPa) than those reported in the literature for histopathologic cirrhosis with chronic hepatitis B (3.67 kPa) and C (4.60 kPa) [28, 29]. These discrepancies probably reflect the fact that the clinically diagnosed liver cirrhosis group in our study included patients with lower grades of histopathologic fibrosis as well as cirrhosis. Although the two MRE sequences yielded similar diagnostic accuracy for the detection of clinical liver cirrhosis, SE-EPI-MRE had higher accuracy for high-risk oesophageal varices than GRE-MRE (AUC = 0.839 vs. 0.752, respectively). This difference is probably due to the exclusion of five patients who failed in GRE-MRE from the generation of the ROC curve.

In our study, iron overload was the most common cause of failure of GRE-MRE (6 of 9). As expected, logistic regression analysis revealed that increased iron content (i.e. decreased  $T2^*$ ) was associated with an increased risk of GRE-MRE failure. However, some patients failed GRE-MRE even without iron overload. In a recent study by Wagner et al. [17], the higher image quality of the SE-EPI-MRE was explained by its shorter acquisition time as well as insensitivity to  $T2^*$  decay. In their study, scan time per acquisition, which is related to respiratory motion artefacts, was longer in SE-EPI-MRE (16 s due to four slices in one acquisition) than GRE-MRE (14 s). Therefore, we believe that scan time should not be considered a sole risk factor of failure for GRE-MRE. In our study, each breath-hold for GRE-MRE (18 s) was longer than the single breath-hold required for SE-EPI-MRE (7 s). Despite the longer breath-hold time in GRE-MRE, there were no failures due to respiratory motion artefacts, which can be easily detected in magnitude images. Therefore, we hypothesize that failures in GRE-MRE, except for cases due to iron overload, are linked to patient-related factors including severe atrophic changes in liver-altering appropriate wave propagation and poor image SNR. Sequence-related factors affecting the quality of wave encoding are SNR in the image phase, which may be higher for SE-EPI than for GRE, and may explain the lower failure rates of SE-EPI-MRE. Wave encoding can be impaired by several patient-related factors (fat interposition) or setup (driver placement and belt tension), but these presumably affected both GRE and SE-EPI equally.

SE-EPI-MRE has several advantages compared to GRE-MRE. In a recent study, SE-EPI-MRE showed better subjective image quality and larger confidence maps in comparison with GRE-MRE [17]. Also, because of its shorter acquisition time, SE-EPI-MRE allows multiple slice acquisition in a single breath-hold, which results in an increased liver coverage. Large areas of coverage for LS measurement are one of the major strengths of MRE compared with other imaging modalities and liver biopsy [4, 30]. With larger confidence maps in SE-EPI-MRE, measured LS values would likely represent a more generalized assessment of diffuse liver disease [17]. In addition, SE-EPI-MRE is less prone to iron deposition or field inhomogeneity-related effects, since SE-EPI is less sensitive to transversal signal relaxation than GRE [31]. In line with this, six patients with iron deposition (i.e. short T2\*) in our study failed only GRE-MRE.

Our study had several limitations. First, our study was limited by its retrospective design. Second, there was no pathologic proof of liver fibrosis, and thus we could not determine the exact performance of MRE for the detection and staging of liver fibrosis. Third, the details of both MRE pulse sequences were not optimized. Fourth, we did not evaluate the image quality of SE-EPI-MRE and GRE-MRE.

In conclusion, we observed excellent reproducibility for LS between SE-EPI-MRE and GRE-MRE at 3 T with no evidence of influence of gadoteric acid administration. We also demonstrated that the failure rate of SE-EPI-MRE is significantly lower than that of GRE-MRE. Thus, SE-EPI-MRE is a better alternative than GRE-MRE, especially in patients with iron deposition, who are likely to fail GRE-MRE.

**Acknowledgements** The authors thank Dr. Takayuki Obata (National Institute of Radiological Sciences, Japan), Dr. Mikio Suga (Chiba University, Japan) and Dr. Takayuki Abe (Siemens Japan SJKK) for their scientific contributions to SE-EPI-MRE. The authors thank the MR radiographers of our unit, Mr. Hyun-Geun Lee, Mr. Dae-Hyun Kim, Mr. Keun-Taek Oh and Mr. Eun-Seong Kim, for technical assistance with MR studies.

#### Compliance with ethical standards

**Guarantor** The scientific guarantor of this publication is Ji Soo Song.

**Conflict of interest** The authors of this manuscript declare no relationships with any companies whose products or services may be related to the subject matter of the article.

**Funding** This paper was supported by the Fund of Biomedical Research Institute, Chonbuk National University Hospital

**Statistics and biometry** No complex statistical methods were necessary for this paper.

**Ethical approval** Institutional review board approval was obtained.

**Informed consent** The requirement for written informed consent was waived for review of patient records and images.

#### Methodology

- retrospective
- observational
- performed at one institution

#### References

1. Martínez SM, Crespo G, Navasa M, Forns X (2011) Noninvasive assessment of liver fibrosis. *Hepatology* 53:325–335
2. Venkatesh SK, Yin M, Ehman RL (2013) Magnetic resonance elastography of liver: technique, analysis, and clinical applications. *J Magn Reson Imaging* 37:544–555
3. Loomba R, Wolfson T, Ang B, Hooker J, Behling C, Peterson M et al (2014) Magnetic resonance elastography predicts advanced fibrosis in patients with nonalcoholic fatty liver disease: a prospective study. *Hepatology* 60:1920–1928
4. Yoon JH, Lee JM, Joo I, Lee ES, Sohn JY, Jang SK et al (2014) Hepatic fibrosis: prospective comparison of MR elastography and US shear-wave elastography for evaluation. *Radiology* 273:772–782
5. Batheja M, Vargas H, Silva AM, Walker F, Chang YH, De Petris G et al (2015) Magnetic resonance elastography (MRE) in assessing hepatic fibrosis: performance in a cohort of patients with histological data. *Abdom Imaging* 40:760–765
6. Yin M, Glaser KJ, Talwalkar JA, Chen J, Manduca A, Ehman RL (2016) Hepatic MR Elastography: clinical Performance in a Series of 1377 Consecutive Examinations. *Radiology* 278:114–124
7. Yoshimitsu K, Mitsufuji T, Shinagawa Y, Fujimitsu R, Morita A, Urakawa H et al (2016) MR elastography of the liver at 3.0 T in diagnosing liver fibrosis grades; preliminary clinical experience. *Eur Radiol* 26:656–663
8. Huwart L, Sempoux C, Salameh N, Jamart J, Annet L, Sinkus R et al (2007) Liver fibrosis: noninvasive assessment with MR elastography versus aspartate aminotransferase-to-platelet ratio index. *Radiology* 245:458–466
9. Wang Y, Ganger DR, Levitsky J, Sternick LA, McCarthy RJ, Chen ZE et al (2011) Assessment of chronic hepatitis and fibrosis: comparison of MR elastography and diffusion-weighted imaging. *AJR Am J Roentgenol* 196:553–561
10. Park HS, Kim YJ, Yu MH, Choe WH, Jung SI, Jeon HJ (2014) Three-Tesla magnetic resonance elastography for hepatic fibrosis: comparison with diffusion-weighted imaging and gadoteric acid-enhanced magnetic resonance imaging. *World J Gastroenterol* 20:17558–17567
11. Venkatesh SK, Yin M, Takahashi N, Glockner JF, Talwalkar JA, Ehman RL (2015) Non-invasive detection of liver fibrosis: MR imaging features vs. MR elastography. *Abdom Imaging* 40:766–775
12. Ronot M, Lambert S, Elkrief L, Doblus S, Rautou PE, Castera L et al (2014) Assessment of portal hypertension and high-risk oesophageal varices with liver and spleen three-dimensional multifrequency MR elastography in liver cirrhosis. *Eur Radiol* 24:1394–1402
13. Shin SU, Lee JM, Yu MH, Yoon JH, Han JK, Choi BI et al (2014) Prediction of esophageal varices in patients with cirrhosis: usefulness of three-dimensional MR elastography with echo-planar imaging technique. *Radiology* 272:143–153
14. Yoon JH, Lee JM, Suh KS, Lee KW, Yi NJ, Lee KB et al (2015) Combined use of MR fat quantification and MR elastography in living liver donors: can it reduce the need for preoperative liver biopsy? *Radiology* 276:453–464
15. Takamura T, Motosugi U, Ichikawa S, Sano K, Morisaka H, Ichikawa T et al (2016) Usefulness of MR elastography for



- detecting clinical progression of cirrhosis from child-pugh class A to B in patients with type C viral hepatitis. *J Magn Reson Imaging*. doi:10.1002/jmri.25182
16. Rump J, Klatt D, Braun J, Warmuth C, Sack I (2007) Fractional encoding of harmonic motions in MR elastography. *Magn Reson Med* 57:388–395
  17. Wagner M, Besa C, Bou Ayache J, Yasar TK, Bane O, Fung M et al (2016) Magnetic resonance elastography of the liver: qualitative and quantitative comparison of gradient echo and spin echo echoplanar imaging sequences. *Investig Radiol*. doi:10.1097/rli.0000000000000269
  18. Motosugi U, Ichikawa T, Sou H, Sano K, Muhi A, Ehman RL et al (2012) Effects of gadoxetic acid on liver elasticity measurement by using magnetic resonance elastography. *Magn Reson Imaging* 30: 128–132
  19. Runge JH, Bohte AE, Verheij J, Terpstra V, Nederveen AJ, van Nieuwkerk KM et al (2014) Comparison of interobserver agreement of magnetic resonance elastography with histopathological staging of liver fibrosis. *Abdom Imaging* 39:283–290
  20. Serai SD, Yin M, Wang H, Ehman RL, Podberesky DJ (2015) Cross-vendor validation of liver magnetic resonance elastography. *Abdom Imaging* 40:789–794
  21. Yasar TK, Wagner M, Bane O, Besa C, Babb JS, Kannengiesser S et al (2015) Interplatform reproducibility of liver and spleen stiffness measured with MR elastography. *J Magn Reson Imaging*. doi: 10.1002/jmri.25077
  22. Hallinan JT, Alsaif HS, Wee A, Venkatesh SK (2015) Magnetic resonance elastography of liver: influence of intravenous gadolinium administration on measured liver stiffness. *Abdom Imaging* 40: 783–788
  23. Stanley DW, Glaser KJ, Yin M, Chen J, Ehman RL (2010) Validity study of spin echo EPI based hepatic MR elastography at 3.0T. 18th Annual Meeting of ISMRM, Stockholm, pp 639
  24. Shi Y, Xia F, Li QJ, Li JH, Yu B, Li Y et al (2016) Magnetic resonance elastography for the evaluation of liver fibrosis in chronic hepatitis B and C by using both gradient-recalled echo and spin-echo echo planar imaging: a prospective study. *Am J Gastroenterol*. doi:10.1038/ajg.2016.56
  25. Bashir MR, Zhong X, Dale BM, Gupta RT, Boll DT, Merkle EM (2013) Automated patient-tailored screening of the liver for diffuse steatosis and iron overload using MRI. *Am J Roentgenol* 201:583–588
  26. Zhong X, Nickel MD, Kannengiesser SA, Dale BM, Kiefer B, Bashir MR (2014) Liver fat quantification using a multi-step adaptive fitting approach with multi-echo GRE imaging. *Magn Reson Med* 72:1353–1365
  27. Kim KY, Song JS, Kannengiesser S, Han YM (2015) Hepatic fat quantification using the proton density fat fraction (PDFF): utility of free-drawn-PDFF with a large coverage area. *Radiol Med* 120: 1083–1093
  28. Chang W, Lee JM, Yoon JH, Han JK, Choi BI, Lee KB et al (2016) Liver fibrosis staging with MR elastography: comparison of diagnostic performance between patients with chronic hepatitis B and those with other etiologic causes. *Radiology*. doi:10.1148/radiol.2016150397:150397
  29. Ichikawa S, Motosugi U, Ichikawa T, Sano K, Morisaka H, Enomoto N et al (2012) Magnetic resonance elastography for staging liver fibrosis in chronic hepatitis C. *Magn Reson Med Sci* 11: 291–297
  30. Bedossa P, Dargere D, Paradis V (2003) Sampling variability of liver fibrosis in chronic hepatitis C. *Hepatology* 38:1449–1457
  31. Huwart L, Salameh N, ter Beek L, Vicaut E, Peeters F, Sinkus R et al (2008) MR elastography of liver fibrosis: preliminary results comparing spin-echo and echo-planar imaging. *Eur Radiol* 18: 2535–2541